PROCEEDINGS A

rspa.royalsocietypublishing.org

Research

Cite this article: Száz D, Farkas A, Barta A, Kretzer B, Egri Á, Horváth G. 2016 North error estimation based on solar elevation errors in the third step of sky-polarimetric Viking navigation. *Proc. R. Soc. A* **472**: 20160171. http://dx.doi.org/10.1098/rspa.2016.0171

Received: 8 March 2016
Accepted: 23 June 2016

Subject Areas:
atmospheric science, optics, sensory biophysics

Keywords:
Viking navigation, sky polarization, solar elevation, sunstone, North estimation

Author for correspondence:
Gábor Horváth
e-mail: gh@arago.elte.hu

Electronic supplementary material is available at http://dx.doi.org/10.1098/rspa.2016.0171 or via http://rspa.royalsocietypublishing.org.

North error estimation based on solar elevation errors in the third step of sky-polarimetric Viking navigation

Dénes Száz[1], Alexandra Farkas[1,2], András Barta[1,3], Balázs Kretzer[1], Ádám Egri[1,2] and Gábor Horváth[1]

[1]Environmental Optics Laboratory, Department of Biological Physics, Physical Institute, Eötvös University, Pázmány sétány 1, 1117 Budapest, Hungary
[2]MTA Centre for Ecological Research, Danube Research Institute, Karolina út 29-31, 1113 Budapest, Hungary
[3]Estrato Research and Development Ltd, Németvölgyi út 91/c, 1124 Budapest, Hungary

GH, 0000-0002-9008-2411

The theory of sky-polarimetric Viking navigation has been widely accepted for decades without any information about the accuracy of this method. Previously, we have measured the accuracy of the first and second steps of this navigation method in psychophysical laboratory and planetarium experiments. Now, we have tested the accuracy of the third step in a planetarium experiment, assuming that the first and second steps are errorless. Using the fists of their outstretched arms, 10 test persons had to estimate the elevation angles (measured in numbers of fists and fingers) of black dots (representing the position of the occluded Sun) projected onto the planetarium dome. The test persons performed 2400 elevation estimations, 48% of which were more accurate than $\pm 1^\circ$. We selected three test persons with the (i) largest and (ii) smallest elevation errors and (iii) highest standard deviation of the elevation error. From the errors of these three persons, we calculated their error function, from which the North errors (the angles with which they deviated from the geographical North) were determined for summer solstice and spring equinox, two specific dates of the Viking sailing period. The range of possible North errors $\Delta\omega_N$ was the lowest and highest at low and

THE ROYAL SOCIETY PUBLISHING

high solar elevations, respectively. At high elevations, the maximal $\Delta\omega_N$ was 35.6° and 73.7° at summer solstice and 23.8° and 43.9° at spring equinox for the best and worst test person (navigator), respectively. Thus, the best navigator was twice as good as the worst one. At solstice and equinox, high elevations occur the most frequently during the day, thus high North errors could occur more frequently than expected before. According to our findings, the ideal periods for sky-polarimetric Viking navigation are immediately after sunrise and before sunset, because the North errors are the lowest at low solar elevations.

1. Introduction

Viking sailors used their extraordinary navigational expertise and skills to cover long distances in the North Atlantic region. During their journeys, they discovered new areas like Iceland and Greenland, where they also established colonies, as well as the coasts of North America [1,2]. To maintain constant trade routes between Scandinavia and their colonies, they needed to keep to very precise sailing routes [3,4]. It is still unclear how they could maintain the correct direction without any advanced navigational tools such as a magnetic compass. According to some theories, they benefited from atmospheric optic navigational cues, for example crepuscular rays [3,5–7] or Arctic mirages [8,9].

According to an old but unproven theory, Vikings used a Sun compass combined with sunstones to orient themselves [10]. The only archaeological finding in connection with Viking navigation stems from 1948, when a fragment of a wooden dial was found in Greenland, under a Benedictine convent in an ancient Viking colony, near the Uunartoq Fjord [11–13]. This fragment turned out to be a remnant from the Viking era, and, according to the most possible assumptions, it was part of a Sun compass, a device used for marine navigation that determines the direction of geographical North with the help of the shadow cast by a vertical gnomon onto the horizontal dial surface in sunshine. Its alternative function and usage was proposed by Bernáth *et al*. [14,15].

Sunstones are referred to in ancient Viking stories, sagas, and are described as tools that can be used to detect the position of the Sun even when it is covered by clouds or fog [7,16,17]. According to the theory, sunstones could possibly be dichroic cordierite, tourmaline and andalusite, for instance, or birefringent calcite (Icelandic spar) [18–25], through which the observer (navigator, always a male in the Viking age) can see the changes in the intensity of the transmitted linearly polarized skylight while he rotates the crystal in front of his eyes. The steps in this sky-polarimetric Viking navigation method are described in detail elsewhere [7,17,26,27].

The three substeps of Viking navigation are briefly the following: (i) Viking navigators determined the direction of skylight polarization in at least two celestial points with the use of two sunstones, which might have been birefringent (e.g. calcite) or dichroic (e.g. cordierite or tourmaline) crystals. Adjusting the sunstone by rotating it in front of his eyes at two different celestial points, the navigator could determine the directions perpendicular to the local direction of skylight polarization shown by the previously engraved straight markings of the sunstones, pointing towards the Sun. (ii) The intersection of the two great celestial circles crossing the sunstones parallel to their engravings gave the position of the invisible Sun even when it was occluded by cloud/fog or below the horizon. (iii) Using the Viking Sun compass, the navigator could derive the geographical Northern direction from the estimated position of the invisible Sun.

This theory is frequently cited and accepted without providing information about its accuracy. Previously, we have measured by imaging polarimetry the atmospheric optical prerequisites of this navigation method under skies with different cloud and fog coverage [7,17,28–30]. The accuracy of the first step has been measured in a laboratory experiment [27] and that of the second step in a planetarium experiment [26]. Now, we have measured the accuracy of the third step in a psychophysical experiment in a planetarium. In the third step, the navigator had to estimate the solar elevation angle of the invisible Sun (occluded by cloud or fog) determined in the first

and second steps. After this third step, the navigator could project the imaginary sunray onto the horizontal surface of the Sun compass [4]. The estimation of the solar elevation was most possibly performed by using numbers of his own fists and fingers to measure it, as described by Bernáth *et al*. [31]. Knowing the solar elevation, the shadow of the occluded Sun had to be replaced by a shadow-stick, as described in detail by Bernáth *et al*. [15,31].

Here, we present the results of our psychophysical planetarium experiment in which we investigated the accuracy of the estimation of virtual solar elevation. Using the obtained error function, we calculated the errors of North determination, assuming that the first and second navigational steps were errorless.

2. Material and methods

(a) Measuring the error of virtual solar elevation

The measurement of the error of virtual solar elevation was performed with 10 male test persons, aged between 24 and 52 years, in the digital planetarium of the Eötvös University in Budapest, Hungary, in autumn 2015. The diameter of the dome at the planetarium is 8 m and a fixed central single-lens Digitarium ε projector (Digitalis Education Solutions Inc., Bremerton, WA, USA) with a circumferential resolution of 2400 pixels was used for projecting pictures onto the dome canvas. The test persons sat in the geometric middle point of the dome, in the immediate vicinity (30 cm) of the planetarium projector with their eye level about 5 cm below the projector lens in order not to be dazzled by the projector and to minimize the parallax error. The measurements by one test person consisted of five 20-minute sessions. To minimize exhaustion and learning of test persons, each session was performed on a different day, so that the test persons could not memorize their previous estimations.

Every session started with a calibration, during which a scale of the elevation angle was projected onto the dome (figure 1*a*,*b*). The scale began at $\theta = 8^\circ$ of elevation above the horizon, because the horizontal circular bottom edge of the planetarium dome, representing the horizon, was 8° above the eye level of the test persons (figure 1*c*). The test person had to stretch out his arm and close his fist with his four fingers (the thumb did not play a role in this measurement) together. Then he started to determine the apparent elevation of his fists and fingers with 1° accuracy up to $\theta = 60^\circ$. According to the method described by Bernáth *et al*. [31], one fist was equal to four fingers and each finger was considered to be of equal width. This process had to be performed with each test person, because their arm length to fist size ratio was slightly different. At the end of each session, the calibration was repeated, thus one test person had 10 calibration data points altogether. These data points were evaluated later by calculating the average and standard deviation of angles for each fist–finger unit.

For the estimation of virtual solar elevation, the experiment leader showed images of a clearly visible black dot (representing the virtual invisible Sun) in front of a white background (figure 1*d*). The azimuthal angles of these dots were the same in every picture, only the elevation angle was varied randomly from $\theta = 8^\circ$ to 55°, thus altogether 48 images were projected randomly during one session. The lower boundary was set to the bottom edge of the dome; dots below this level could not have been projected. An upper boundary of 55° was set, because at the 61st latitude, along which the Vikings sailed the most frequently, the maximal elevation cannot be higher than 52.5° [4,27]. The test persons had to estimate the elevation of the projected black dot by using their fists and fingers without knowing the true elevation angle. At the end of the five sessions, the test person had five estimated values for each elevation in fist–finger units. Thus, altogether $5 \times 48 \times 10 = 2400$ elevation estimations were performed by the 10 test persons.

The evaluation of the results was performed with custom-written software according to the following method. (i) First, we evaluated the calibration results for the test persons separately by calculating the average angle and standard deviation for each fist–finger combination. (ii) Based on the calibration, we determined the estimated elevation in degrees of a given fist–finger value. Thus, we obtained a list of the true elevation values and the estimated values belonging to them

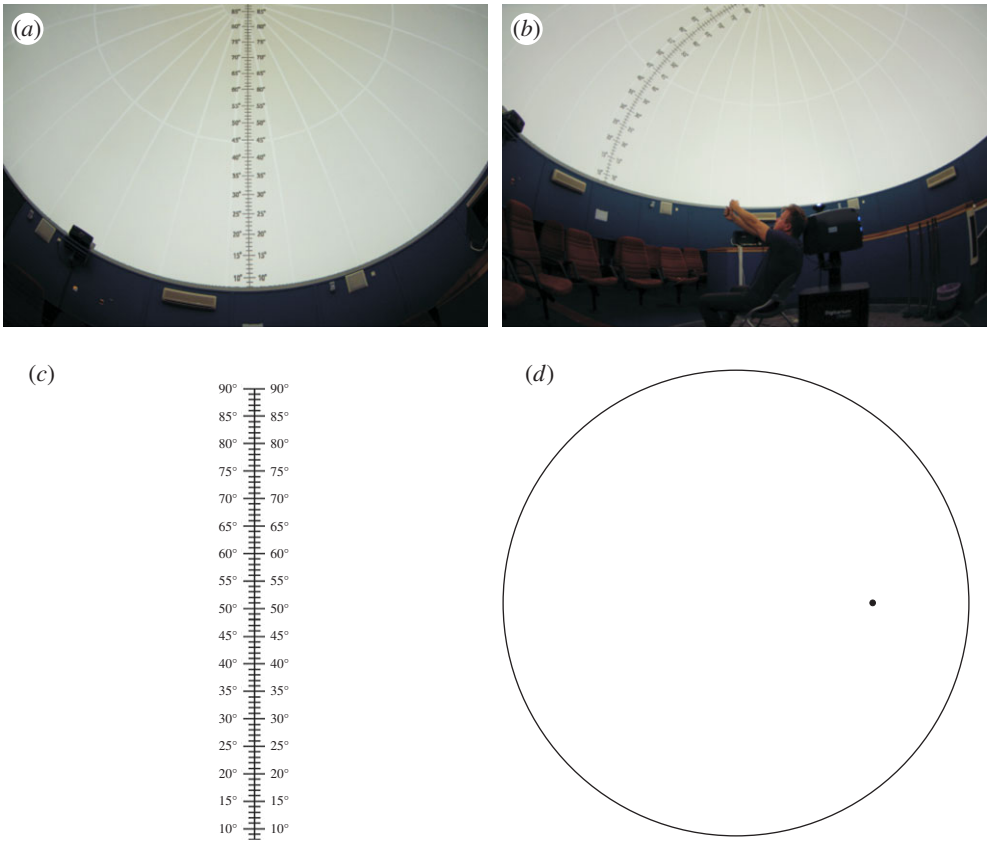

Figure 1. (*a*) Wide-angle photograph of the calibration image that test persons saw projected onto the planetarium canvas. (*b*) Photo of the calibration process. The test person sat in the middle point of the planetarium under the dome and tried to perform the calibration using his fists and fingers. (*c*) Image of the calibration scale which began at an elevation $\theta = 8^\circ$, because the horizontal circular bottom edge of the planetarium dome, representing the horizon, was 8° above the eye level of the test persons. (*d*) An example of the projected measurement situation. The test person was shown a black dot representing the Sun, and he had to estimate the elevation using only his fists and fingers. (Online version in colour.)

in degrees (°), for each test person. (iii) Knowing these values, we calculated the errors with sign (+, −) to mark whether the test person over- or underestimated the true value. As we had five estimations for each true value, we calculated the average μ and standard deviation σ of these errors.

As the results of the test persons were very different, the average of the values for 10 test persons would be far from a real-life situation, where the navigator obviously had the best navigational skills. Thus, to characterize the performance of the test persons, we introduced the cumulated elevation error $\Sigma = \Sigma_{i=1}^{i=48}[|\mu(\theta_i)| + \sigma(\theta_i)]$, meaning the sum of the absolute values of the average $\mu(\theta_i)$ plus standard deviation $\sigma(\theta_i)$ for every θ_i elevation. The sense of calculating the cumulated elevation error is the following: after we evaluated the results of elevation estimation of the 10 test persons, each person had five measurement data points for each θ_i elevation. The error for one elevation was characterized by the average $\mu(\theta_i)$ for these data and their standard deviation $\sigma(\theta_i)$. To compare the performance of a given test person, we summarized these parameters describing the error at θ_i, resulting in the cumulated elevation error Σ described above. The index i runs from 1 to 48, because the elevation θ_i was measured from 8° to 55° by 1° steps. The person with the highest Σ value was, by definition, the worst navigator, the person with the lowest Σ value was the best navigator.

Table 1. Numerical values of the parameters and asymptotic errors of the error function $f(x) = ax^b$ obtained for the elevation error of the three selected test persons in §3.

	parameters			
test person	a	$\pm\Delta a$	b	$\pm\Delta b$
1	0.11	0.07	0.78	0.16
7	1.23	0.43	0.35	0.10
10	0.03	0.01	1.59	0.07

We created a histogram by dividing the elevation errors into 0.5° intervals and counted the occurrences of the cases within the 2400 estimations. Then we fitted a Gaussian function to the symmetric part of the distribution around the peak to quantify the position of the distribution peak.

(b) Deriving the North error

To determine the North error ω_N, we selected three test persons: test person 1 had the lowest Σ value, test person 10 had the highest Σ value and test person 7 had the highest standard deviation σ of the μ values. The results of other test persons fell between the two extremes (test persons 1 and 10). For these three selected test persons, first we determined the error function, which is a continuous function that gives the elevation error for any elevation value for $0° < \theta < 52.5°$ (possible real-life elevation situations at the 61st latitude [4,27]). To do this, we calculated $|\mu(\theta_i)| + \sigma(\theta_i)$ (average + standard deviation) for each elevation angle θ_i, which characterized the maximum possible error of a given test person at elevation θ_i, then we fitted a power function $f(x) = ax^b$ with the method of least squares, where a and b are the fitting parameters, the values of which can be seen in table 1. The error function was determined for test persons 1, 7 and 10.

The North errors were calculated with custom-developed software as follows. (i) The error function gave the elevation error E for a given elevation angle θ. This can be either positive or negative (over- or underestimation), thus we get a range $\theta - E < \theta_{Est} < \theta + E$ in which the solar elevation is estimated (figure 2*a*). (ii) If we project the tip of the gnomonic shadow onto the horizontal surface of the Viking Sun compass (figure 2*b*), the shadow length is the longest for the lowest estimated elevation $S_{\theta-E}$ and the shortest for the highest estimated elevation $S_{\theta+E}$. This defines a range in which the shadow of the gnomon tip can fall. From now on, we will use only these two boundary values. (iii) We used the same two gnomonic lines, for summer solstice and spring equinox at the 61st latitude, as in Száz *et al*. [27]. The previously derived uncertainty in the shadow length results in the error of North determination. If the shadow tip belonging to the true Sun position falls exactly on the gnomonic line, the North determination is correct. In the case of over- or underestimation of the solar elevation, the angles with which the Sun compass has to be rotated until the shadow tip falls on the gnomonic line give the North errors (figure 2*c*). Thus, the uncertainty range of shadow length defines an error range of the North determination. (iv) Because one gnomonic shadow can reach the gnomonic line twice a day (in the forenoon and in the afternoon), we split the gnomonic lines into a forenoon half and an afternoon half. (v) At spring equinox, the maximum possible solar elevation is 29° [27]. In this case, the calculations were performed for $0° < \theta < 29°$. (vi) At low elevations, values of $\theta - E$ could be negative. In these cases, instead of negative values 0 was taken into consideration. (vii) At high elevations, values of $\theta + E$ could go over 29° and 52.5° in the case of spring equinox and summer solstice, respectively. Because, in these cases, the gnomonic shadow is too short and does not reach the gnomonic line, they had to be omitted.

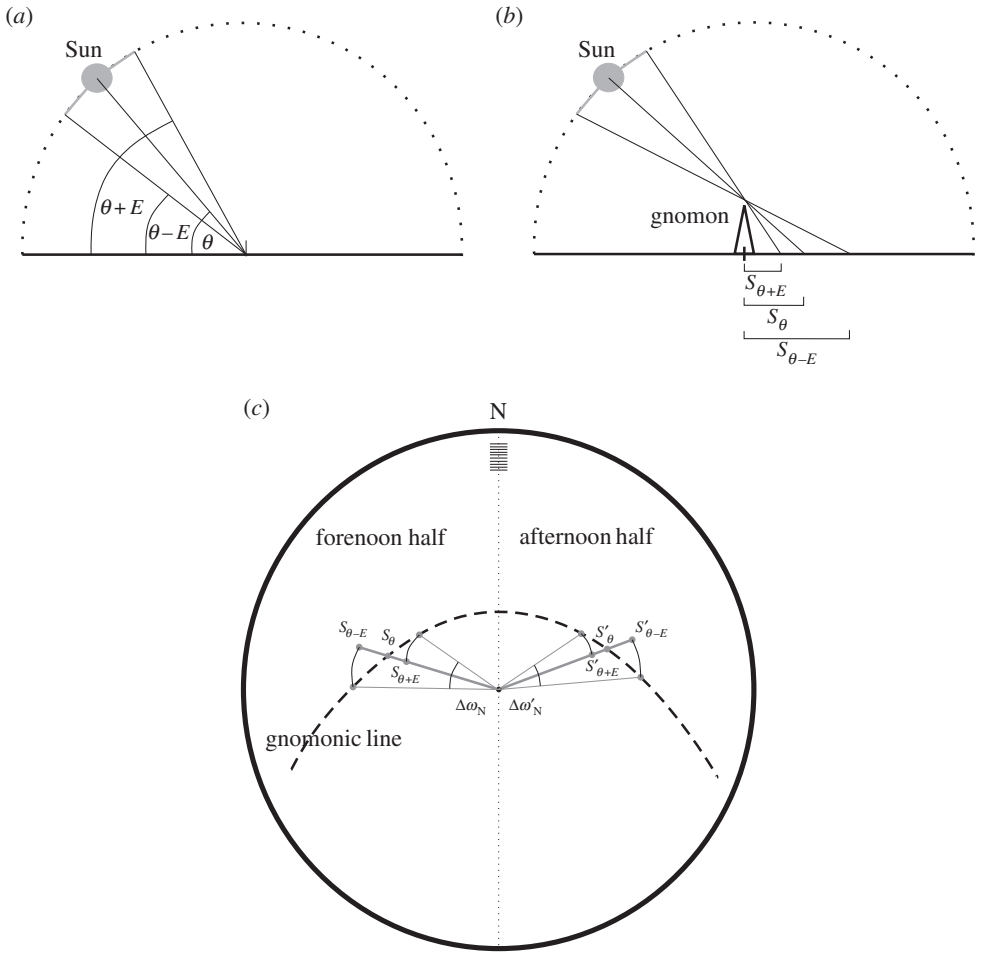

Figure 2. Steps of the North error determination calculated with custom-developed software. (*a*) The error functions (§3) gave the elevation error E for a given θ elevation. This can be positive or negative (over- or underestimation); thus, we get a range $\theta - E < \theta_{\mathrm{Est}} < \theta + E$ in which the Sun is estimated. (*b*) If we project the Sun's shadow onto the horizontal surface of the Sun compass, the shadow length is the longest for the lowest estimated elevation $S_{\theta-E}$ and the shortest for the highest estimated elevation $S_{\theta+E}$. This defines a range in which the gnomonic shadow length can fall. (*c*) The degree with which the Sun compass has to be rotated until the shadow tip falls on the gnomonic line gives the North error. The uncertainty range of the shadow length defines an error range in the North determination. One shadow tip can reach the gnomonic line twice a day: in the forenoon and in the afternoon. This defines a range in the forenoon ($\Delta\omega_{\mathrm{N}}$) and in the afternoon ($\Delta\omega'_{\mathrm{N}}$) in which all the North errors fall that can be derived from the estimated Suns. The North errors were determined for the selected test persons in four cases: (i) summer solstice in the forenoon, (ii) summer solstice in the afternoon, (iii) spring equinox in the forenoon, and (iv) spring equinox in the afternoon.

The North errors were determined for test persons 1, 7 and 10 in the following four cases: (i) summer solstice in the forenoon, (ii) summer solstice in the afternoon, (iii) spring equinox in the forenoon, and (iv) spring equinox in the afternoon.

To obtain information about how often a given elevation value during the sailing period occurs, we created histograms in AlgoNet (http://www.estrato.hu/algonet) for the whole navigation period (from spring equinox to autumn equinox) and for the days of spring equinox and summer solstice, separately. We chose an elevation interval of 1° to create the histograms which were calculated for the latitude 60°21′55″ N of Hernam (nowadays Bergen, Norway), the Vikings' onetime most important sailing latitude connected to Hvarf in South Greenland [4,17]. During calculations, atmospheric refractions were also taken into consideration [32].

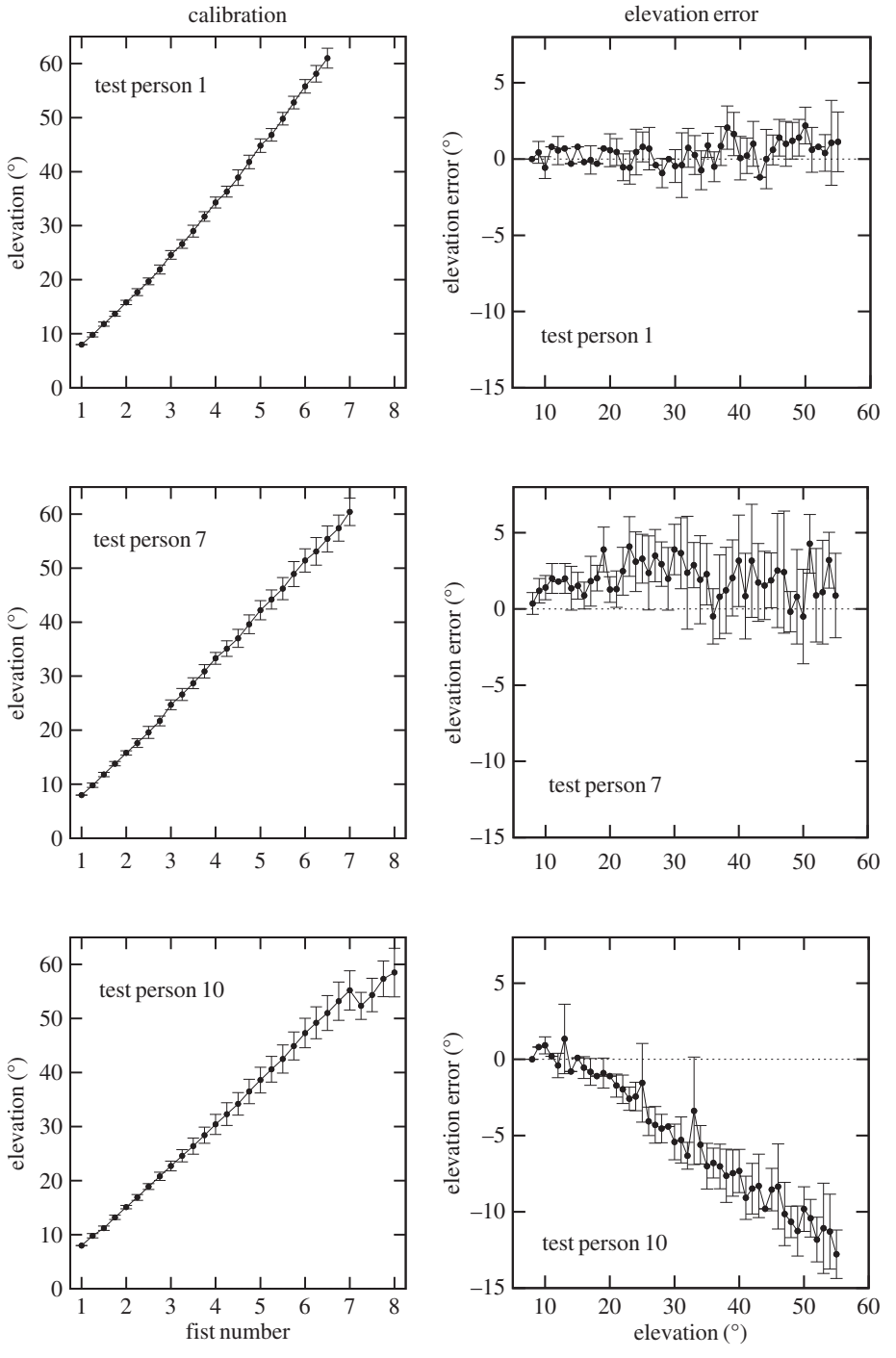

Figure 3. Calibration and elevation results for the three selected test persons (test person 1 with the lowest Σ, test person 7 with the highest standard deviation σ of μ, and test person 10 with the highest Σ) in our planetarium experiment. The lines are not fits, rather they just join the data points.

3. Results

The results of the calibration and the average values with standard deviations of the elevation error are shown in figure 3 for the three selected test persons 1, 7 and 10, and in the electronic

Table 2. The cumulated elevation error Σ for the 10 test persons and their rank (1 for the best and 10 for the worst navigator). The three selected persons with the lowest Σ (test person 1), highest Σ (test person 10) and highest standard deviation σ of μ (test person 7) are marked in bold italic. The percentages in the brackets mean the relative error of the test persons compared with that of the worst navigator (test person 10).

test person	cumulated elevation error Σ(°)	rank
1	***79.3*** (***25.2%***)	***1***
2	115.2 (36.6%)	7
3	85.3 (27.1%)	2
4	149.9 (47.6%)	8
5	111.8 (35.5%)	5
6	88.0 (27.9%)	3
7	***193.8*** (***61.5%***)	***9***
8	110.2 (35.1%)	4
9	113.6 (36.0%)	6
10	***315.1*** (***100.0%***)	***10***

supplementary material, figures S1 and S2, for all the 10 test persons individually. It can be generally observed that the standard deviation increases with the solar elevation. Some test persons had a break in the monotonously growing calibration curve (test person 5 in the electronic supplementary material, figure S1, and test persons 8 and 10 in the electronic supplementary material, figure S2), the causes of which are described in the Discussion. The elevation errors also show an increasing tendency in standard deviation as a function of the virtual solar elevation. For some test persons, clear overestimations (test person 7 in the electronic supplementary material, figure S2) and underestimations (test person 4 in the electronic supplementary material, figure S1, and test persons 8 and 10 in the electronic supplementary material, figure S2) of the virtual solar elevation can be observed. The cumulated elevation error Σ is summarized in table 2, where the results of test persons 1, 7 and 10 are marked in bold italic. Σ for the worst navigator (test person 10 with the highest Σ) was almost four times as much as that for the best navigator (test person 1 with the lowest Σ), while test person 7 (with the highest standard deviation σ of μ) had 2.5 times higher errors than the best navigator.

In the case of the North error determination, figure 4 shows the error functions $f(x) = ax^b$ for test persons 1, 7 and 10. In figure 4, the functional form fitted to the elevation errors is rather arbitrary and is motivated to catch the trend of the measured data to quantify a continuous curve for interpolation between data points. The North errors obtained from error propagation are visualized in figure 5. Increasing solar elevation results in a growing range of North error $\Delta\omega_N$ in which the North error values can fall. The maximum of these ranges with the corresponding minimum and maximum North error values and the elevation where this maximum is reached can be seen in figure 5 for the different cases and the three selected test persons (navigators). The maximal range of $\Delta\omega_N$ was twice as high for the worst navigator (test person 10) and 1.4 times as high for test person 7 as that for the best navigator (test person 1) at summer solstice, while at spring equinox these ratios were 1.8 and 1.7, respectively. The elevations for the maximum ranges were the lowest in the worst case, the highest in the best case, and they were between the two extremes for test person 7. The numerical values of these ranges are listed in table 3. This means that navigators with worse results can determine even the lower solar elevations less accurately. The North error values calculated for the forenoon and afternoon half of the same gnomonic line are around the same value, but with opposite sign (as seen in figure 5). Logically, this is to be expected, because the Sun compass needs to be rotated in opposite directions in the forenoon and in the afternoon if the solar elevation is the same.

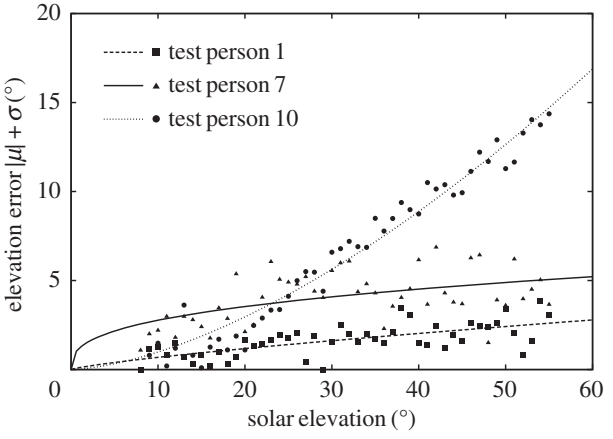

Figure 4. Error functions fitted in the form of $f(x) = ax^b$ to the elevation measurement results of the three selected navigators 1, 7 and 10. Table 1 contains the numerical values of the fitting parameters.

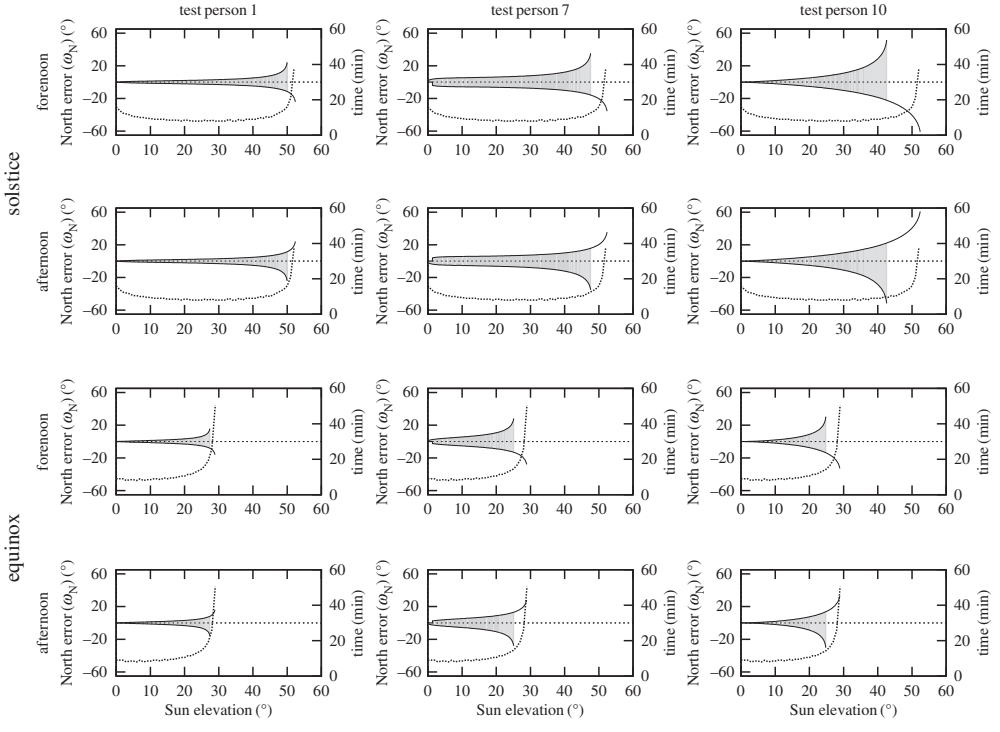

Figure 5. North error results obtained from the error propagation of the elevation errors for the three selected test persons 1, 7 and 10. The following dates were studied: summer solstice in the forenoon (row 1), summer solstice in the afternoon (row 2), spring equinox in the forenoon (row 3), spring equinox in the afternoon (row 4). The upper and lower curve enclosing a given grey wedge area is the upper limit and lower limit of possible North errors as a function of the Sun's elevation, respectively. For further explanation, see Materials and methods (§2b). The curves below the grey wedge areas show the frequency of occurrence of a specific elevation of the Sun throughout a day at spring equinox (figure 6*a*) or summer solstice (figure 6*b*).

Figure 6 shows the frequency of solar elevation values with a 1° interval at spring equinox (figure 6*a*), summer solstice (figure 6*b*) and during the whole sailing period (from spring equinox to autumn equinox, figure 6*c*). The frequency of solar elevations during the sailing period has two peaks: one at low elevations when the Sun is close to the horizon, and one at around 29°, which

Table 3. The minimum and maximum North error values ω_N for the maximum North error ranges $\Delta\omega_N$ and the solar elevation θ_S at which it is reached for test persons 1, 7 and 10. Sol, summer solstice; Equ, spring equinox; am, forenoon; pm, afternoon.

	test person 1			test person 7			test person 10		
time	min–max ω_N (°)	$\Delta\omega_N$ (°)	θ_S (°)	min–max ω_N (°)	$\Delta\omega_N$ (°)	θ_S (°)	min–max ω_N (°)	$\Delta\omega_N$ (°)	θ_S (°)
Sol am	−11.5 to +24.1	35.6	50	−15.8 to +35.1	50.9	47.6	−22.2 to +51.6	73.8	42.6
Sol pm	−24.1 to +11.5	35.6	50	−35.1 to +15.8	50.9	47.6	−51.6 to +22.2	73.8	42.6
Equ am	−8.1 to +15.7	23.8	27.4	−13.1 to +28.1	41.2	25.1	−13.7 to +30.3	44.0	24.8
Equ pm	−15.8 to +8.1	23.9	27.4	−28.0 to +13.1	41.1	25.1	−30.2 to +13.7	43.9	24.8

is the elevation maximum at spring and autumn equinox [27]. These elevations occur every day during the sailing period. The decreasing tendency at elevations higher than 29° indicates that higher elevations occur on fewer days as we approach the summer solstice and the Sun is at 52.5° elevation only at the solstice [27]. At the specific dates of the solstice and equinox, the elevations around the maximum last for the longest time.

Figure 7 shows the histograms of the occurrences of the elevation errors. The distribution peak belonged to the 0–0.5° interval and 48% of all elevation errors were included in the interval from −1° to +1°. The asymmetry of the distribution shows that the range of underestimations was higher, but the numbers of under- and overestimations were around the same: 1083 underestimations (below 0–0.5°) and 1053 overestimations (above 0–0.5°) were performed. The expected value of the Gaussian curve fitted to the symmetric part of the peak region was $\mu = 0.32°$, which corresponds to the histogram data. The standard deviation of the fitting was $\sigma = 1.74°$. Hence, approximately half (48%) of all estimations were more accurate than ±1°. Approximately the same numbers of over- and underestimations means that both unintentional effects of tiring could occur equally often. The high number of the relatively low elevation errors also implies that, if it cannot be decided who the best navigator is, it is worth choosing several navigators instead of accidentally selecting a possibly poor one. However, Viking navigator candidates surely had undergone thorough training and selection before they fulfilled their job; thus, it is a realistic assumption that a qualified Viking navigator had better results than our best-performing test person 1.

4. Discussion

The tendency that for higher solar elevations we got higher standard deviations of the elevation error can be observed in both the calibration and the measurement parts of our psychophysical experiment. This is to be expected because of the cumulative nature of the navigator's estimation process. Since estimation is based on sequential fist–finger steps, the error itself will be cumulative, as can be seen from our results, and is probably accentuated by the tiring of arm muscles: the test persons had to stretch out their arms and measure the elevation with their fists and fingers by putting the two fists above each other. At lower solar elevations, up to two fists (*ca* 16°), this task was easy, but at higher elevations the fists could accidentally move downwards, owing to gravitation and the tiring of arm muscles, causing an elevation error. The more times a test person had to put one fist above the other, the stronger this effect could be. The gradual tiring of the test person's arms could also elicit this effect. Because this downwards movement of the arms is completely random, this effect was different in the five measurement sessions, causing the increasing standard deviation of the elevation errors. The systematic overestimation of some test persons (which was also described by Bernáth *et al*. [15,31] and Farkas *et al*. [26]) can also be explained by the same effect. When the fists of the test person move downwards, he systematically reported a higher elevation value than the true one, as seen for test person 7 in the electronic supplementary material, figure S2, for example. This unfortunate effect could not be eliminated

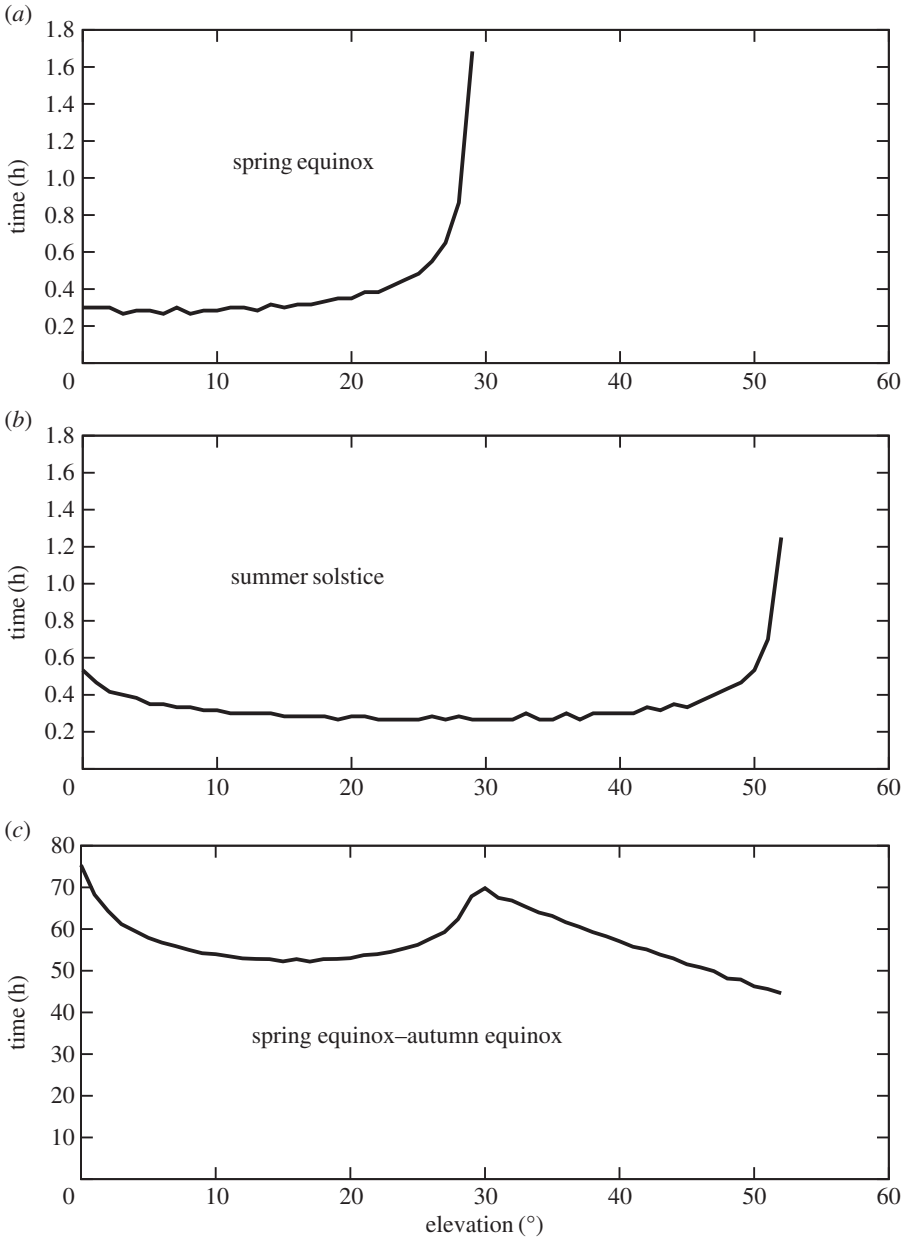

Figure 6. Histograms of solar elevation occurrence throughout a day at spring equinox (*a*), summer solstice (*b*) and the whole navigation season (from spring equinox to autumn equinox, *c*), computed for Bergen (latitude 60°21′55″ N), along the most frequent Viking sailing route. The elevation interval to create the histograms was 1°.

from the experiment, and it surely contributed to the real-life situation, because this effect can more easily occur on board a moving Viking ship. In a real-life scenario of Viking navigation, when the ship, and thus also the horizon, was continuously swinging due to undulation, it would have been difficult to use any device that could help the navigators in reducing estimation errors due to muscle stress and/or an occasional slip of their arms and fists.

The systematic underestimation of the solar elevation in our planetarium experiment can have an alternative explanation: when the test person at higher elevations raises his arms, he does not keep them outstretched straight, but instead bends them in slightly (e.g. because of tiring). This reaction can be unintentional. If his arms are bent in, his fists are closer to his eyes and thus

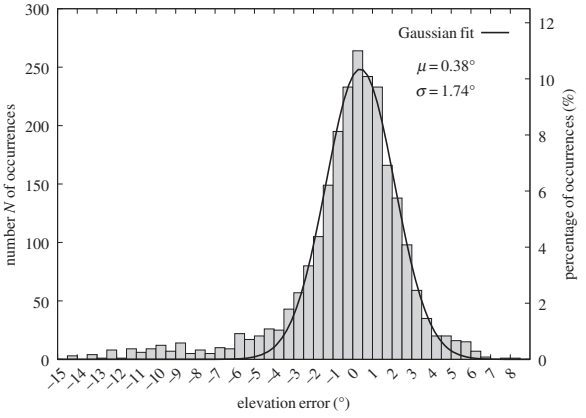

Figure 7. Histogram for the occurrences of elevation errors and Gaussian fitting characterized by the mean μ and the standard deviation σ. The error interval for creating the histogram was 0.5°.

optically seem bigger than when they are outstretched. A bigger fist means a higher elevation value, thus the test person reports systematically lower numbers of fist-and-finger than when his arms were outstretched. Because the calibration process is shorter, this effect happens only rarely or does not occur at all during that part of the measurement. Thus, according to the calibration, the given fist–finger value belongs to a lower solar elevation than the true one. This effect can be observed in the case of the worst test person 10 in figure 3 and of some others (test person 4 in the electronic supplementary material, figure S1, as well as test persons 8 and 10 in the electronic supplementary material, figure S2).

Some test persons had a break in the monotonously growing calibration curve (test person 5 in the electronic supplementary material, figure S1, and test persons 8 and 10 in the electronic supplementary material, figure S2). This can be the effect of tiring of the arm muscles during the calibration process. When the test person got tired, his hands could accidentally move downwards, or he might have put his hands down for a moment. These are unintentional natural reactions to tiring that the test persons could not eliminate during the measurements. This effect also increases the elevation error; thus, a navigator who gets tired less easily can measure more accurately.

The results of North error determination show that the maximal elevation error and the range of North errors $\Delta\omega_N$ increase as a function of solar elevation. The latter finding is the consequence of error propagation. It is a logical conclusion that the most ideal period of the day for navigation is when the possible North error is minimal, i.e. immediately after sunrise and before sunset. During these periods, the systematic error effects are also minimal. In figure 5, it is clearly seen, however, that for test person 7 the range of North errors is higher even for lower solar elevations, which is the cause of the large standard deviation in his elevation errors. The possible reason for this large standard deviation can be the lack of experience, because test person 7 participated for the first time in such a psychophysical navigational experiment. Obviously, if a navigator has more experience in estimating the solar elevation, the standard deviation will be lower.

From the frequency of solar elevations θ_S (figure 6), it turned out that the highest elevations can last as long as low elevations. This means that, according to our results, the time period when the North errors can be high are rather long. This is especially true for the spring equinox and summer solstice, where the maximum solar elevations last for the longest time. If the navigation happens around noon when θ_S is highest, it is worth navigating several times a day, equally distributed in the forenoon and in the afternoon. Then, the net navigation error will be around zero on average, because the Sun compass needs to be rotated in opposite directions in the forenoon and in the afternoon if the length of the gnomonic shadow is the same, and, if it is erroneous, the North error will also have an opposite sign in the forenoon and afternoon.

During the sailing period, low solar elevations occur the most often, therefore it is advisable to navigate immediately after sunrise and before sunset, because the North errors at low solar elevations are the lowest in every examined case in our experiment. This can be performed quite often based on the data in figure 6*c*.

The Vikings' sailing routes were characterized by a frequent weather situation when the Sun around the horizon was covered by clouds or thick fog, but the zenith above the navigator's head remained clear. According to Száz *et al*. [27], measurements with dichroic cordierite and tourmaline or birefringent calcite sunstone crystals in the highly polarized clear parts of the sky can result in an accurate determination of the Sun's position. According to our results presented here, in these situations, the estimation of solar elevation adds the least error to the accuracy of the whole sky-polarimetric Viking navigation. To quantify the navigation error, if none of the three navigational steps are errorless, will be the scope of our further research.

Finally, we emphasize that in our experiment the test persons had to estimate the elevation angles of easily seen black dots projected onto a bright planetarium dome (figure 1*d*), whereas in reality a Viking navigator had to perform such an estimation with regard to an actually invisible Sun. The latter is obviously a more difficult task. Thus, the elevation errors presented in this work underestimate the real errors of the third step of sky-polarimeric Viking navigation. On the other hand, Viking navigators were surely more experienced in the estimation of elevation angles than our test persons.

5. Conclusion

On the basis of the results of our psychophysical planetarium measurements we conclude the following:

— The standard deviation of elevation errors increases with solar elevation.
— The average of elevation errors shows systematic over- or underestimations for certain test persons.
— 48% of all elevation estimations were more accurate than $\pm 1^\circ$.
— The $\Delta\omega_N$ ranges of possible North errors obtained from error propagation increase with the solar elevation.
— The maximal $\Delta\omega_N$ was twice as high for test person 10 (73.8°) and 1.4 times as high for test person 7 (50.9°) as for test person 1 (best Viking navigator) (35.6°) at summer solstice, while at spring equinox these ratios were 1.8 (44.0°) and 1.7 (41.2°), respectively (23.8° for test person 1).
— Low solar elevations occur almost as frequently as high elevations during the sailing period of the Vikings, while at summer solstice and spring equinox the highest elevations are the most frequent ones.
— The ideal periods for navigation are immediately after sunrise and before sunset when the solar elevation is low and thus $\Delta\omega_N$ is the lowest.

We need to emphasize that these conclusions are true only for the third step of sky-polarimetric Viking navigation, assuming that the first and second steps are errorless. In a following paper, we will study how the errors of the three steps of sky-polarimetric Viking navigation add up under different sky conditions. For that study, we will use the error functions of the first and second steps measured earlier [26,27] along with the polarization patterns of numerous (more than 1000) different skies measured by full-sky imaging polarimetry.

Authors' contributions. D.S., A.F. and G.H. designed the experiment; D.S., A.F. and Á.E. performed the experiment; D.S., A.B. and Á.E. did the programming; D.S. and B.K. analysed the data; D.S., A.F. and G.H. wrote the paper and answered the comments of the reviewers.

Competing interests. The authors declare no competing or financial interests.

Funding. This work was supported by grant OTKA K-105054 (Full-Sky Imaging Polarimetry to Detect Clouds and to Study the Meteorological Conditions Favourable for Polarimetric Viking Navigation) received by G.H. from the Hungarian Science Foundation. A.F. was supported by the Hungarian Templeton Program.

Acknowledgements. G.H. thanks the Alexander von Humboldt Foundation, Germany, for donating equipment. We thank the 10 test persons for their co-operation. We are grateful to Prof. Kristóf Petrovay, head of the Department of Astronomy of Eötvös University (Budapest), who made the planetarium at Eötvös University available for our experiment. We are grateful to two anonymous reviewers for their constructive and positive comments. The opinions expressed in this publication are those of the authors and do not necessarily reflect the views of Templeton World Charity Foundation, Inc.

References

1. McGovern TH. 1990 The archaeology of the Norse North Atlantic. *Annu. Rev. Anthropol.* **19**, 331–351. (doi:10.1146/annurev.an.19.100190.001555)
2. Ingstad H, Ingstad AS. 2000 *The Viking discovery of America. The excavation of a Norse settlement in L'Anse aux Meadows, Newfoundland*. St. John's, Newfoundland: Breakwater Book Ltd.
3. Thirslund S. 1997 Sailing directions of the North Atlantic Viking age (from about the year 860 to 1400). *J. Navig.* **50**, 55–64. (doi:10.1017/S0373463300023584)
4. Thirslund S. 2001 *Viking navigation: sun-compass guided Norsemen first to America*. Humlebaek, Denmark: Gullanders Bogtrykkeri a-s, Skjern.
5. Roslund C, Beckman C. 1994 Disputing Viking navigation by polarized skylight. *Appl. Opt.* **33**, 4754–4755. (doi:10.1364/AO.33.004754)
6. Barta A, Horváth G, Meyer-Rochow VB. 2005 Psychophysical study of the visual sun location in pictures of cloudy and twilight skies inspired by Viking navigation. *J. Opt. Soc. Am. A* **22**, 1023–1034. (doi:10.1364/JOSAA.22.001023)
7. Horváth G, Farkas A, Bernáth B. 2014 Sky-polarimetric Viking navigation. In *Polarized light and polarization vision in animal sciences*, ch. 25 (ed. G Horváth), pp. 603–635. Berlin, Germany: Springer.
8. Sawatzky HL, Lehn WH. 1976 The Arctic mirage and the early North Atlantic. *Science* **192**, 1300–1305. (doi:10.1126/science.192.4246.1300)
9. Lehn WH, Schroeder II. 1979 Polar mirages as aids to Norse navigation. *Polarforschung* **49**, 173–187.
10. Ramskou T. 1967 Solstenen. *Skalk* **2**, 16–17.
11. Solver CV. 1953 The discovery of an early bearing-dial. *J. Navig.* **6**, 294–296. (doi:10.1017/S0373463300027314)
12. Taylor EG, May WE, Motzo RB, Lethbridge TC. 1954 A Norse bearing-dial? *J. Navig.* **7**, 78–84. (doi:10.1017/S0373463300036225)
13. Thirslund S. 1991 A presumed sun compass from Narsarsuaq. In *The church topography of the eastern settlement and the excavation of the Benedictine convent at Narsarsuaq in the Uunartoq Fjord* (ed. CL Vebæk), pp. 65–71. Monographs on Greenland, vol. 278: Man & Society, vol. 14. Copenhagen, Denmark: Museum Tusculanum Press.
14. Bernáth B, Blahó M, Egri Á, Barta A, Horváth G. 2013 An alternative interpretation of the Viking sundial artefact: an instrument to determine latitude and local noon. *Proc. R. Soc. A* **469**, 20130021. (doi:10.1098/rspa.2013.0021)
15. Bernáth B, Farkas A, Száz D, Blahó M, Egri Á, Barta A, Åkesson S, Horváth G. 2014 How could the Viking Sun compass be used with sunstones before and after sunset? Twilight board as a new interpretation of the Uunartoq artefact fragment. *Proc. R. Soc. A* **470**, 20130787. (doi:10.1098/rspa.2013.0787)
16. Foote PG. 1956 Icelandic sólarsteinn and the Medieval Background. *Arv. J. Scand. Folklore* **12**, 26–40.
17. Horváth G, Barta A, Pomozi I, Suhai B, Hegedüs R, Åkesson S, Meyer-Rochow B, Wehner R. 2011 On the trail of Vikings with polarized skylight: experimental study of the atmospheric optical prerequisites allowing polarimetric navigation by Viking seafarers. *Phil. Trans. R. Soc. B* **366**, 772–782. (doi:10.1098/rstb.2010.0194)
18. Walker J. 1978 The amateur scientist: more about polarizers and how to use them, particularly for studying polarized sky light. *Sci. Am.* **238**, 132–136. (doi:10.1038/scientificamerican0178-132)
19. Schaefer BE. 1997 Vikings and polarization sundials. *Sky Telesc.* **93**, 91–94.
20. Wild W, Fromme B. 2007 Der Sonnenstein der Wikinger: navigation mit polarisierten Himmelsicht. *Praxis der Naturwissenschaften - Physik in der Schule* **56**, 33–38.
21. Ball P. 2011 Material witness: a light compass? *Nat. Mater.* **10**, 814. (doi:10.1038/nmat3153)

22. Hawthorne CF, Dirlam DM. 2011 Tourmaline the indicator mineral: from atomic arrangement to Viking navigation. *Elements* **7**, 307–312. (doi:10.2113/gselements.7.5.307)
23. Karman SB, Diah SZM, Gebeshuber IC. 2012 Bio-inspired polarized skylight-based navigation sensors: a review. *Sensors* **12**, 14 232–14 261. (doi:10.3390/s121114232)
24. Ropars G, Gorre G, Le Floch A, Enoch J, Lakshminarayanan V. 2012 A depolarizer as a possible precise sunstone for Viking navigation by polarized skylight. *Proc. R. Soc. A* **468**, 671–684. (doi:10.1098/rspa.2011.0369)
25. Le Floch A, Ropars G, Lucas J, Wright S, Davenport T, Corfield M, Harrisson M. 2013 The sixteenth century Alderney crystal: a calcite as an efficient reference optical compass? *Proc. R. Soc. A* **469**, 20120651. (doi:10.1098/rspa.2012.0651)
26. Farkas A, Száz D, Egri Á, Blahó M, Barta A, Nehéz D, Bernáth B, Horváth G. 2014 Accuracy of sun localization in the second step of sky-polarimetric Viking navigation for north determination: a planetarium experiment. *J. Opt. Soc. Am. A* **31**, 1645–1656. (doi:10.1364/JOSAA.31.001645)
27. Száz D, Farkas A, Blahó M, Barta A, Egri Á, Kretzer B, Hegedüs T, Jäger Z, Horváth G. 2016 Adjustment errors of sunstones in the first step of sky-polarimetric Viking navigation: studies with dichroic cordierite/tourmaline and birefringent calcite crystals. *R. Soc. open sci.* **3**, 150406. (doi:10.1098/rsos.150406)
28. Hegedüs R, Åkesson S, Horváth G. 2007 Polarization patterns of thick clouds: overcast skies have distribution of the angle of polarization similar to that of clear skies. *J. Opt. Soc. Am. A* **24**, 2347–2356. (doi:10.1364/JOSAA.24.002347)
29. Hegedüs R, Åkesson S, Wehner R, Horváth G. 2007 Could Vikings have navigated under foggy and cloudy conditions by skylight polarization? On the atmospheric optical prerequisites of polarimetric Viking navigation under foggy and cloudy skies. *Proc. R. Soc. A* **463**, 1081–1095. (doi:10.1098/rspa.2007.1811)
30. Barta A *et al.* 2014 Polarization transition between sunlit and moonlit skies with possible implications for animal orientation and Viking navigation: anomalous celestial twilight polarization at partial moon. *Appl. Opt.* **53**, 5193–5204. (doi:10.1364/AO.53.005193)
31. Bernáth B, Blahó M, Egri Á, Barta A, Kriska G, Horváth G. 2013 Orientation with a Viking sun-compass, a shadow-stick, and two calcite sunstones under various weather conditions. *Appl. Opt.* **52**, 6185–6194. (doi:10.1364/AO.52.006185)
32. Meeus JH. 1991 *Astronomical algorithms*. Richmond, VA: Willmann-Bell, Incorporated.